Power distribution analysis for multiple modulation formats in an all-optical sampling wavelength division multiplexing system

Hai Yu (于 海), Hongwei Chen (陈宏伟)*, Minghua Chen (陈明华), and Shizhong Xie (谢世钟)

Tsinghua University, Department of Electronic Engineering National Laboratory for Information Science and Technology (TNList), Beijing 100084, China

**Corresponding author: chenhw@tsinghua.edu.cn*

Received May 6, 2013; accepted August 2, 2013; posted online September 29, 2013

An optimal power distribution analysis for an all-optical sampling orthagonal frequency division multiplexing (OFDM) scheme with multiple modulation formats including differential phase shift keyed (DPSK), differential quadrature phase shift keyed (DQPSK), and non-return-to-zero (NRZ) is proposed. The noise tolerances of different modulation formats are analyzed, and the optimal input power ratio between phase and intensity modulation formats for the best overall receiving performance is investigated under unchanged total input power. Moreover, this scheme can seamlessly coexist with the traditional WDM channel.

OCIS codes: 060.4510, 060.4230, 060.4080.
doi: 10.3788/COL201311.100604.

Optical orthogonal frequency division multiplexing (O-OFDM) method is widely applied in many applications[1] because of its high spectral efficiency, robustness against both chromatic dispersion and polarization mode dispersion, as well as natural compatibility with digital signal processing-based implementation[2].

Realizing Fourier transform in the optical domain to generate an all-optical OFDM signal maximizes the use of high-speed and large-bandwidth optical transmission. A real-time all-optical Fourier transform receiver enabling a line rate of 10.8 and 26 Tb/s with cascaded delay interferometers (DIs) and high-speed optical gates has been recently proposed[3,4]. A 1.5-Tb/s super-channel is generated using all-optical OFDM and dual-polarization 16QAM modulation without a guard interval[5]. A novel method of all-optical OFDM signal generation with optical cyclic postfixes (OCPs) and real-time direct detection using optical Fourier-transform filters based on fiber Bragg gratings (FBGs) is proposed[6]. This method realizes all-optical implementations in both transmitter and receiver ends and avoids constructing a complex structure for coherent detection and optical gates for synchronization. An all-optical sampling OFDM (AOS-OFDM) system performance analysis is given under different numbers of channels, modulation formats, and pulse widths[7]. An experiment on an all-optical sampling AOS-OFDM transmission system with five subcarriers non-return-to-zero (NRZ) modulation is demonstrated[8]. All above mentioned methods of generating an all-optical OFDM signal considers only the same modulation format, and the situation using multiple modulation formats for an AOS-OFDM system has not yet been discussed. Considering the requirements of different data rates, costs, and performances for different users, multiple modulation format multiplexing can satisfy application diversity especially in an optical OFDM-PON system. Such an AOS-OFDM system can flexibly adjust the number of subcarriers and generate the signal meeting wave division multiplexing (WDM) bandwidth requirements. This system can also be embedded into a WDM channel and transmitted simultaneously with other WDM channels.

In this letter, the situation with only phase modulation formats including differential phase shift keyed (DPSK) and differential quadrature phase shift keyed (DQPSK) is discussed. The modulation format NRZ is added to examine how intensity and phase modulation formats influence each other when the total input power is unchanged. Finally, the optimal power distribution for different modulation formats for obtaining the best receiving performance of the entire all-optical sampling OFDM (AOS-OFDM) system is determined.

At the transmitter, ultra-short optical pulses are used as samples to conduct an all-optical discrete fourier transform (DFT)/inverse discrete fourier (IDFT) process through MUX-FBG and DMUX-FBG; thus, adding optical cyclic prefixs (CPs) to OFDM signals in the optical domain and having more DFT points in one compact structure are easy. Such an AOS-OFDM signal with OCPs is generated. Figure 1 shows the schematic of the proposed AOS-OFDM scheme with multiple modulation formats.

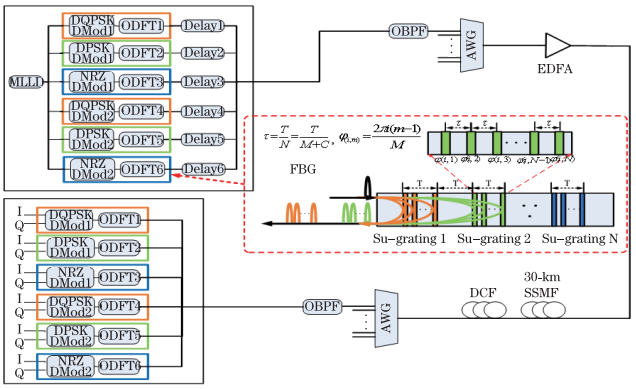

Fig. 1. AOS-OFDM scheme frame with multiple modulation formats.

At the receiver, a real-time direct-detection technique consisting of both optical Fourier-transform filters based on FBGs, as well as differential and balance detection, is used to simplify the receiver structure. Thus, the electrical bottlenecks of digital-to-analog/analog-to-digital conversion and digital signal processing are avoided. To realize the flexibility of an AOS-OFDM scheme, different modulation formats are used for different subcarriers to achieve variable data rates and different receiving performances.

Figure 1 shows a 10-GHz ultra-short pulse source from a mode-locked laser diode split into six parts. The three modulation formats DQPSK, DPSK, and NRZ are applied interleaved to the six parts. The bandwidth of each part is 10 GHz, so the bit rates are 20, 10, and 10 Gb/s for DQPSK, DPSK, and NRZ, respectively. They pass through corresponding optical modulators and inverse discrete Fourier transform based on FBGs, and an AOS-OFDM signal with multiple modulation formats is generated. The symbol period is 100 ps. The number of optical samples is 16, and the number of cyclic postfix is 4. Delay lines are used to ensure that all six subcarriers are synchronized in the time domain. Then, the AOS-OFDM signal passes through an optical band-pass filter and sent into 30-km standard single mode fiber (SSMF) and dispersion compensating fiber (DCF). The DCF is still needed to compensate for the chromatic dispersion (CD) that optical CPs cannot compensate for. At the receiver, the OFDM signal is split into six parts again, and each part passes through corresponding discrete Fourier transform modules, as well as DQPSK, DPSK, and NRZ demodulators. The interleaved arrangement of modulation formats is considered for its universality, as shown in Fig. 1. Simulation software used includes Optisystem 7 and Matlab 7. The main parameters are shown in Table 1.

Figure 2 shows the spectra of DQPSK and AOS-OFDM signal with four subcarriers, including DQPSK and DPSK modulation formats. The spectrum of DPSK is similar to that of DQSPK. The spectrum interval of optical OFDM subcarriers is 10 GHz. The input power of each subcarrier is −2.6 dBm.

Figure 3 shows that the transmission performance of the DPSK modulation format is obviously better than that of DQPSK because the former has a larger phase interval and higher noise tolerance. Then, the intensity modulation format NRZ is added, and the input power of each subcarrier is the same (−2.6 dBm).

Table 1. System Configuration

Parameter	Value
Pulse Shape	Gaussian
Pulse Width	2 ps
Signal Period	100 ps
BPF Shape	Second-order Gaussian
Symbol Rate	10 G/s
Dispersion of SMF	17 ps/(nm·km)
Loss of SMF	0.2 dB/km
Fiber Length	30 km
Detector Responsivity	1 A/W
Dark Current	10 nA
Thermal Noise	1×10^{-24} W/Hz

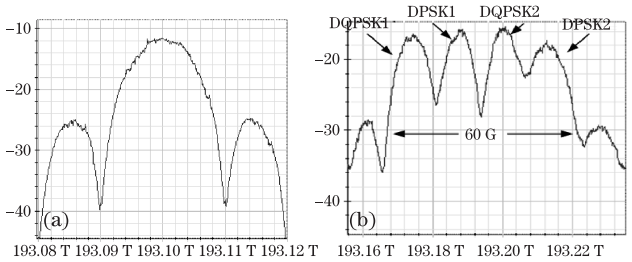

Fig. 2. Spectrx of (a) DPQSK and (b) all-optical OFDM signal with DPSK and DQPSK modulation formats.

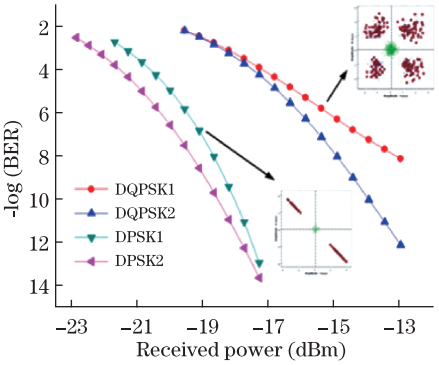

Fig. 3. Bit error rate (BER) curves of DQPSK and DPSK modulation formats.

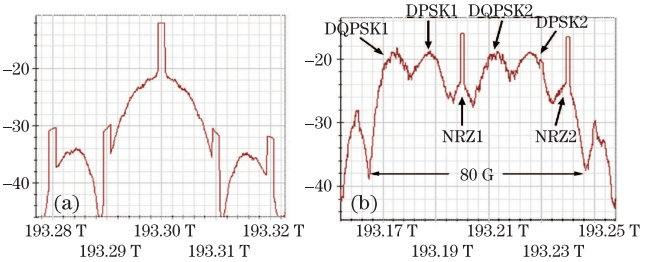

Fig. 4. Spectrum of AOS-OFDM signal with DQPSK, DPSK, and NRZ modulation formats.

Figure 4(a) shows the spectrum of NRZ modulation format, and obvious high-power spectrum components exist in the major and side lobes. The high-power spectrum component in the side lobe is about 4 dBm. Figure 4(b) shows the spectrum of the AOS-OFDM signal with three modulation formats interleaved.

As shown in Fig. 5, the receiving performance between DQPSK and DPSK are similar but obviously poorer than that of NRZ when the input power of the three modulation formats is the same (−2.6 dBm). The optical NRZ signal consists of a series of optical sampling pulses obtained using FBGs, and the spectrum of the NRZ modulation format has high power lines in the major and side bands, as shown in Fig. 4(a). This phenomenon results in cross-talk to orthogonal subcarriers and degrades receiving performance. When the signal-to-noise ratio (SNR) of phase modulation formats decreases, the bit error rate (BER) between intensity and phase modulation formats is obviously different, although the BERs of all phase modulation formats are similar to one another. Figure 5 mainly shows the BER difference between phase and intensity modulation formats to explain how the intensity

modulation format strongly influences phase modulation formats when the input power is a specific value. The BER curves change when the input power of all modulation formats is some other value.

Under the same input power of each subcarrier, the performance of modulation format NRZ is better than those of DQPSK and DPSK. To reduce the influence of cross-talk, the power of the NRZ subcarriers should be reduced. The input power of both DPSK and DQPSK is still −2.6 dBm, and the input power of NRZ is reduced to −10.8 dBm.

Figure 6 shows that the receiving performance of phase modulation formats including DQPSK and DPSK is obviously better than that of NRZ, which is opposite of the result shown in Fig. 5. It shows that if the input power of intensity modulation format NRZ is properly reduced, the influence of cross-talk decreases. Thus, an optimal power distribution for obtaining the best receiving performance for the entire AOS-OFDM system must exist.

We assume that the total input power is −3.1 dBm and unchanged. We only adjust the input power ratio between DPSK/DQPSK and NRZ, where we consider the entire input power of phase modulation formats including DPSK and DQPSK together against the input power of the NRZ modulation format. The $\mathrm{BER_{Total}}$ measuring the receiving performance of the entire AOS-OFDM system in simulation is obtained by calculating the error vector magnitude of each symbol.

Figure 7 shows that the receiving performance curve is approximately a parabola when the input power ratio

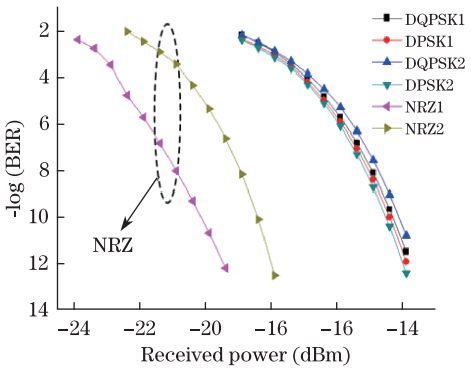

Fig. 5. BER curves when the input powers of the three modulation formats are the same (−2.6 dBm).

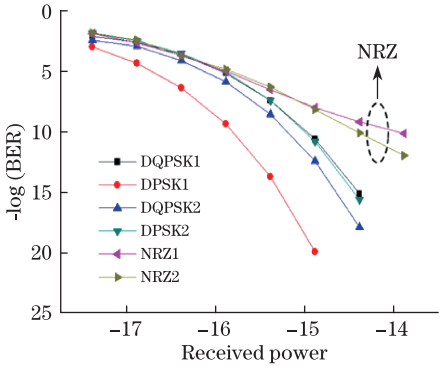

Fig. 6. BER curve when the input power of DPSK and DQPSK is –2.6 dBm and the input power of NRZ is –10.8 dBm.

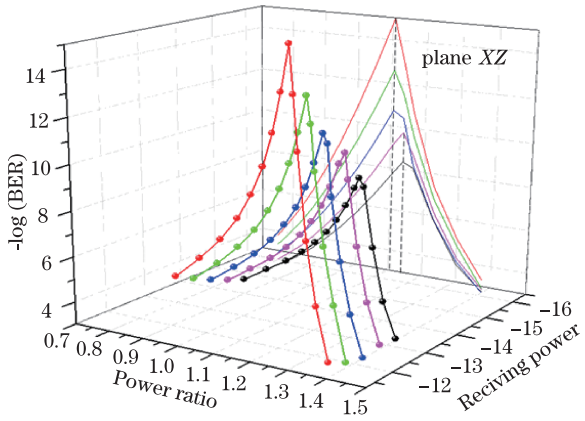

Fig. 7. (Color online) BER curve of different input power distributions.

changes. The best power ratio of the first red curve in Fig. 7 is about 1.107, which means that the input power of the phase modulation format should be properly larger than that of the intensity modulation format to reduce cross-talk from subcarriers with intensity modulation format. Thus, for the three different modulation formats, the best input power distribution can be found to maximize the receiving performance of the entire AOS-OFDM system.

The projections of each curve are shown in plane XZ of Fig. 7. As the total receiving power decreases, the total BER increases and so does the best input power ratio. This phenomenon is due to the fact that when the receiving power decreases, the more complex phase modulation format like DQPSK needs a larger input power to improve the SNR of its own channel to achieve the best receiving performance of the entire AOS-OFDM system.

In conclusion, a novel power distribution analysis for an AOS-OFDM scheme with multiple modulation formats including DPQSK, DPSK, and NRZ is proposed. Given the high-power spectral components in the side lobe from the intensity modulation format NRZ, the phase modulation format needs more input power to overcome the cross-talk and achieve better overall receiving performance. Different input power distributions for subcarriers result in different receiving performances of the entire AOS-OFDM system. Under the condition that the total input power is unchanged, the optimal input power ratio between the phase modulation and intensity modulation formats for the best receiving performance is found. As the total receiving power decreases, the optimal power ratio increases because a more complex modulation format needs more input power to improve the SNR.

This work was supported by the National Natural Science Fundation of China (Nos. 60932004, 61132004, and 61090391) and the Program for New Century Excellent Talents in University (No. NCET-10-0520).

References

1. E. Giacoumidis, J. Wei, X. Yang, A. Tsokanos, and J. Tang, IEEE Photon. J. **2,** 130 (2010).

2. W. Shieh, X Yi, Y Ma, and Q Yang, J. Opt. Network. **7,** 234 (2008).
3. D. Hillerkuss, T. Schellinger, R. Schmogrow, M. Winter, T. Vallaitis, R. Bonk, A. Marculescu, J. Li, M. Dreschmann, J. Meyer, S. Ben Ezra, N. Narkiss, B. Nebendahl, F. Parmigiani, P. Petropoulos, B. Resan, K. Weingarten, T. Ellermeyer, J. Lutz, M. Möller, M. Hübner, J. Becker, C. Koos, W. Freude, and J. Leuthold, in *Optical Fiber Communication Conference, OSA Technical Digest (CD)* PDPC1 (2010).
4. D. Hillerkuss, R. Schmogrow, T. Schellinger, M. Jordan, M. Winter, G. Huber, T. Vallaitis, R. Bonk, P. Kleinow, F. Frey, M. Roeger, S. Koenig, A. Ludwig, A. Marculescu, J. Li, M. Hoh, M. Dreschmann, J. Meyer, S. Ben Ezra, N. Narkiss, B. Nebendahl, F. Parmigiani, P. Petropoulos, B. Resan, A. Oehler, K. Weingarten, T. Ellermeyer, J. Lutz, M. Moeller, M. Huebner, J. Becker, C. Koos, W. Freude, and J. Leuthold, Nature photonics **5,** 364 (2011).
5. Y. Huang, Z. Wang, M. Huang, Y. Shao, and T. Wang. J. Lightwave Technol. **29,** 3838 (2010).
6. H. Chen, M. Chen, and S. Xie, J. Lightwave Technol. **27,** 4848 (2009).
7. H. Ye, H. Chen, C. Tang, M. Chen, and S. Xie, Chin. Opt. Lett. **9,** 010603 (2011).
8. X. Gu, H. Chen, M. Chen, and S. Xie, Chin. Opt. Lett. **10,** 020601 (2012).